Thermal-Fluid Flow Transport Phenomenon over Slot-Perforated Flat Plates Placed in Narrow Channel [*]

Shuichi Torii[†]
Kumamoto University, Kumamoto, 860-8555, JAPAN

and
Wen-Jei Yang[‡]
University of Michigan, Ann Arbor, Michigan, 48109, USA

A numerical study is performed to investigate unsteady, two-dimensional, incompressible laminar flow over both sides of a slot-perforated flat surface, which is placed in a narrow channel. Emphasis is placed on the effect of the blockage factor, i.e., the ratio of plate thickness, δ, to channel width, W, on the heat transfer performance and the velocity and thermal fields. It is found from the study that: (i) when the slot width is increased, the alternating change in the fluid flow disturbs the thermal boundary layer formed along the plate and induces mixing of the upper and lower streams of the plate downstream from the slot, resulting in an amplification of heat transfer performance; (ii) heat transfer performance at the rear plate is induced with an increase in slot-width and Re; and (iii) by contrast, heat transfer performance is attenuated with an increase in the blockage factor, whose effect becomes larger in the lower region of the Reynolds number.

Nomenclature

B	=	channel length, m
d	=	slot width, m
h	=	local heat transfer coefficient on the plate, W/m^2/K, $= \dfrac{\lambda \left[\partial T / \partial y \right]}{T_w - T_{inlet}}$
k_q	=	blockage factor, δ/W
L	=	length of plate, m
Nu	=	local Nusselt number on the plate, $h\delta/\lambda$
$\overline{Nu}$	=	time-averaged Nusselt number on the plate
P, ΔP'	=	pressure and dimensionless pressure drop, $= \Delta P/(0.5\rho u_m^2)$, respectively
Re	=	Reynolds number, $u_m\delta/\nu$
t	=	time, sec.
T	=	temperature, K
U_i	=	velocity component in i directions, m/s
U	=	velocity component in x direction, m/s
u_m	=	inlet fluid velocity, m/s
V	=	velocity component in y direction, m/s
x_i	=	i coordinate, m
ΔX, ΔY	=	mesh size, m
x, y	=	coordinate, m
W	=	channel width, m
α	=	thermal diffusivity, m^2/s

β	=	coefficient
ρ	=	density, kg/m^3
ν	=	molecular viscosity, m^2/s
δ	=	plate thickness, m
λ	=	thermal conductivity, W/m/K
θ	=	dimensionless temperature, $\theta = \dfrac{T - T_{inlet}}{T_w - T_{inlet}}$

Subscripts

| inlet | = | inlet |
| w | = | wall surface of the plate |

I.   Introduction

The heat exchanger is an essential unit in heat extraction and recovery systems. With increasing emphasis on economic and energy saving considerations, a great deal of research effort is devoted to develop more efficient heat-transfer surfaces. In the design of advanced heat exchangers, louver-fins, strip-fins, wavy-fins and perforated-fins are widely used to achieve high heat transfer efficiency and compactness. A comparison of performances among these surfaces was made by Wong et al.[1]. Kays[2] reported that perforation results in a substantial increase in heat-transfer performance without introducing a pronounced form drag. Heat exchangers with perforated fins may be made either in small size and light weight as air-cooled condensers or in large size as air-cooled heat exchangers. This viewpoint was supported by some investigators[1,3].

In general, perforated plates may be employed as an extended surface for internal cooling of turbine blades. They are compact and high in heat-transfer performance induced by boundary layer interruption due to perforations without the salient penalty of the form drag[4-9]. Liang[10] and Liang et al.[11] studied the effects of geometry and arrangement of the perforations on fluid flow behavior and disclosed that the ratio of slot length, in the flow direction, to its thickness plays a very important role in flow behavior. In order to investigate the effects of the Reynolds number and the ratio of the slot width, d, to the plate thickness, δ, on the velocity field, the corresponding numerical analysis was carried out by Torii and Yang[12,13]. They reported that the flow pattern between two plates placed in a free stream or two-dimensional channel can be classified into four categories depending on the combination of Re and d/δ. In particular, at a certain combination of Re and d/δ, an alternating crossing of flow of the fluid streams takes place through the slot from one side to the other side of the plate in the flow direction, so that the heat transfer performance from a surface wall of the rear plate is intensified[14]. Amon and Mikic[15] performed numerical investigation of the flow pattern and forced convective heat transfer in slotted channels, in which numerical results are compared with the results with plane-channel flow. They disclosed that over a certain

Reynolds number the flow exhibits laminar self-sustained oscillations, which cause significant heat transfer enhancement. Suzuki et al.[16] and Nigen and Amon[17] dealt with thermal fluid flow transport phenomenon in a plane channel with an in-line fin array and in a grooved channel, respectively. They reported that heat transfer performance is induced due to the self-sustained oscillatory flow. Heat transfer enhancement by the use of slots in channels with uniformly surface-mounted blocks was investigated by Kim and Anand[18]. They dealt with steady two-dimensional laminar flow and disclosed that cooling performance of slotted channels is improved with an increase in slot size.

Both in industrial heat exchangers and in most experimental rigs, the tubes are placed in channels. The effect of the channel walls is expressed by the blockage factor, which is the ratio of the cylinder diameter to the channel width. A higher blockage factor leads to a higher velocity outside the boundary layer, and to different distributions of pressure and velocity on the cylinder circumferences. Consequently, variations of the shell-cylinder distances lead to change in the local heat transfer. The effect of the blockage factor on heat transfer performance around the cylinder in the channel was summarized by Zukauskas and Ziugzda[19]. By contrast, the corresponding effect on heat transfer from the perforated plates placed in a channel has not been considered.

The present study investigates unsteady thermal and fluid flow transport phenomena over both sides of a slot-perforated surface, which is placed in the narrow channel. Emphasis is placed on the effect of the blockage factor, kq on heat transfer performance and velocity and thermal fields. In this study the flow is assumed to be two dimensional, to keep the computational time manageable. Three-dimensional computations, in general, will require extensive CPU times to conduct parametric tests such as those conducted here. Thus, the effect of three dimensionality, which arises due to either secondary instabilities or end walls, is not taken into account.

II.   Conservation Equations and Numerical Method

The present study deals with a forced flow over a single-slot perforated surface heated with constant wall temperature in the channel, which consists of two plain straight plates (i.e., the front and rear plates), of length, L, and thickness, $\delta\Box\Box$ aligned in the flow direction with a spacing of d. Here two plates are set at y=W/2. Figure 1 depicts the proposed physical model and the coordinate system. The following assumptions are imposed in the formulation of the problem: incompressible, laminar, unsteady flow; constant fluid properties; uniform inlet velocity and uniform inlet fluid temperature; and negligible axial conduction (due to the high Peclet number). Under these

assumptions, the simplified governing equations for mass, momentum and energy read:

$$\frac{\partial U_i}{\partial x_i} = 0, \tag{1}$$

$$\frac{\partial U_i}{\partial t} + U_j \frac{\partial U_i}{\partial x_j} = -\frac{1}{\rho}\frac{\partial P}{\partial x_i} + v\frac{\partial}{\partial x_j}\left(\frac{\partial U_i}{\partial x_j}\right), \tag{2}$$

and

$$\frac{\partial T}{\partial t} + U_j \frac{\partial T}{\partial x_j} = \alpha\frac{\partial}{\partial x_j}\left(\frac{\partial T}{\partial x_j}\right), \tag{3}$$

respectively. Initially, the fluid is quiescent and a uniform temperature at T=T$_{inlet}$. Then, the plate surface temperature is suddenly changed to T=T$_w$. Non-slip condition is employed at the plate surface and the channel walls. At the exit, the boundary conditions for the dependent variables are obtained by setting the first derivatives in the axial direction equal to zero. This is because the same use in other flow conditions is permissible for computational convenience if the outlet boundary is located in a flow region, which is sufficiently far downstream from the region of interest. Notice that the above boundary condition at the exit is strictly valid only when the flow is fully developed.

The discretization method employed in the present study uses a finite difference formulation and the discretized forms of the above governing equations read as:

$$U_{i,j}^{n+1} = U_{i,j}^n + \Delta t\left[\frac{1}{\Delta X}\left(P_{i,j}^n - P_{i+1,j}^n\right) - FUX^n - FUY^n + VISX^n\right] \tag{4}$$

$$V_{i,j}^{n+1} = V_{i,j}^n + \Delta t\left[\frac{1}{\Delta Y}\left(P_{i,j}^n - P_{i,j+1}^n\right) - FVX^n - FVY^n + VISY^n\right] \tag{5}$$

$$T_{i,j}^{n+1} = T_{i,j}^n + \Delta t\left[-FTX^n - FTY^n + VIST^n\right] \tag{6}$$
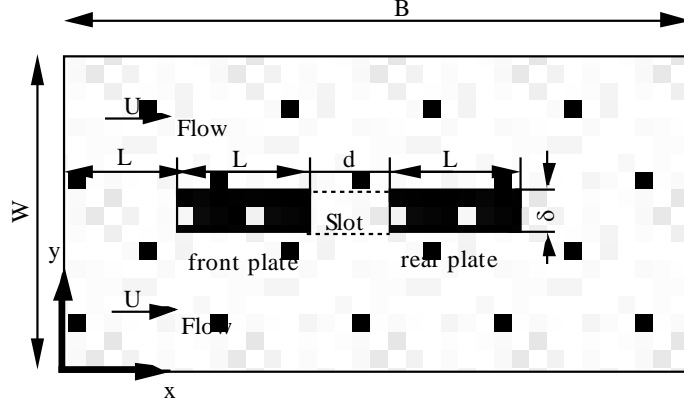
Fig. 1 A schematic of physical system and coordinate.

The subscript and superscript correspond to the cell location and time level, respectively. A detailed description of the above discretization method and FUX^n, FUY^n, $VISX^n$, FVX^n, FVY^n, and $VISY^n$ in Eqs. (4) and (5), are available in the literatures[20,21] and thus are not repeated here. FTX^n, FTY^n, and $VIST^n$ in Eq. (6) are expressed as:

$$FTX^n = \frac{1}{4\Delta X}[(U_{i,j}^n + U_{i,j+1}^n)(T_{i,j}^n + T_{i+1,j}^n) + \beta|U_{i,j}^n + U_{i,j+1}^n|(T_{i,j}^n - T_{i+1,j}^n)$$
$$-(U_{i-1,j}^n + U_{i-1,j+1}^n)(T_{i,j-1}^n + T_{i,j}^n) - \beta|U_{i-1,j}^n + U_{i-1,j+1}^n|(T_{i-1,j}^n - T_{i,j}^n)] \tag{7}$$

$$FTY^n = \frac{1}{4\Delta Y}[(V_{i,j}^n + V_{i+1,j}^n)(T_{i,j}^n + T_{i,j+1}^n) + \beta|V_{i,j}^n + V_{i+1,j}^n|(T_{i,j}^n - T_{i,j+1}^n)$$
$$-(V_{i,j+1}^n + V_{i+1,j-1}^n)(T_{i,j-1}^n + T_{i,j}^n) - \beta|V_{i,j-1}^n + V_{i+1,j-1}^n|(T_{i,j-1}^n - T_{i,j}^n)] \tag{8}$$

$$VIST^n = \alpha[\frac{1}{\Delta X^2}(T_{i+1,j}^n - 2T_{i,j}^n + T_{i-1,j}^n) + \frac{1}{\Delta Y^2}(T_{i,j+1}^n - 2T_{i,j}^n + T_{i,j-1}^n)] \tag{9}$$

The system variables P, U, V and T are calculated with a staggered grid proposed by Harlow and Welch[20]. Here, $P_{i,j}^n$ is pressure at center of cell (i,j) at time level n, $U_{i,j}^n$ is x-direction velocity at middle of right size of cell (i,j) at time level n, $V_{i,j}^n$ is y-direction velocity at middle of top size of cell (i,j) at time level n, and $T_{i,j}^n$ is temperature at center of cell (i,j) at time level n. The processes involved in completing one calculation cycle at an arbitrary time-step are as follows: (i) by solving Eqs. (4)-(6) for U, V and T, subject to the appropriate boundary conditions, the new velocities, which involve the values for the contributing pressure and velocities at the precious time-step, are predicted for the entire mesh to be solved; (ii) these velocities are iteratively adjusted to satisfy the continuity equation, Eq. (1), by making appropriate changes in the cell pressures, that is, each cell in the iteration is considered

successively and is given a pressure change, δp, that drives its instantaneous velocity divergence to zero[22];

$$\delta P = -\frac{\frac{1}{\Delta X}\left(U_{i,j} - U_{i-1,j}\right) + \frac{1}{\Delta Y}\left(V_{i,j} - V_{i,j-1}\right)}{\left|2\Delta t\left(\frac{1}{\Delta X^2} + \frac{1}{\Delta Y^2}\right)\right|} \qquad (10)$$

(iii) when convergence has been reached with a maximum relative change in the values between successive iterations of less 10^{-4}, i.e., $\frac{1}{\Delta X}\left(U_{i,j} - U_{i-1,j}\right) + \frac{1}{\Delta Y}\left(V_{i,j} - V_{i,j-1}\right) \leq 10^{-4}$, the velocity and pressure fields are determined at the advanced time level and are used as starting values at next time-step. These processes are repeated until t reaches a prescribed time, say, t=120 sec after the calculation is initiated. Note that at this time, the thermal transport phenomenon becomes periodic, that is, a steady time-periodic solution is obtained, as shown in the following.

The grid system is changed from 200x400 to 400x800 to obtain a grid-independent solution. Numerical computation was performed on a personal computer at time interval Δt=0.00001 sec. Here, the maximum time interval employed is determined to ensure the numerical stability. Based on the dataset obtained here, visualization of the flow and thermal fields is carried out using a commercially available 2-D graphics software tool.

In general, heat transport phenomenon in a channel flow is affected by three dimensionless parameters, i.e., Re ($=u_m\delta/\nu$), Pr, and k_q. In the present study, L/δ is fixed at 2, and water is used as the working fluid (Pr=0.71), while Re is ranged from 100 to 1200, and k_q is varied from 0.05 to 0.50. d/δ is fixed at 3.0. Note that for d/δ=3.0, the alternating change in the fluid flow disturbs the thermal boundary layer formed along the plate and induces mixing of the upper and lower streams of the plate downstream from the slot, resulting in an amplification of heat transfer performance[23].

Simulations with grids of various degrees of coarseness, as mentioned earlier, were conducted to determine the required resolution for grid-independent solutions. Throughout the Reynolds number range considered here, the maximum relative error was estimated to be about 2% by comparing the solutions on regular and fine grids with twice the grid points. Although a few solutions were computed with half the time step to ensure consistency and time-step independence, there was no substantial discrepancy between two different time intervals.

III.   Results and Discussion

The structure of the flow over the single-slot perforated plate and the wake of the rear plate are discussed through the use of computed instantaneous velocity vectors. Figure 2, for Re=120 and t=100 sec., depicts the

instantaneous maps of fluctuating velocity vector for the different blockage factor. Notice that velocity components are normalized by dividing by inlet velocity. Figures 2(a)-(c) show the numerical results at k_q=0.1, k_q=0.2, and k_q=0.5, respectively. The corresponding temperature distributions, i.e., isotherms, are illustrated in Fig. 3, in which θ=1 and 0 correspond to the heated-plate temperature and the fluid temperature in free stream, respectively. It is observed in (a) and (b) of Figs. 2 and 3 that (i) mixing of the upper and lower streams of the plate downstream from the slot is stimulated, and (ii) this increase induces the alternating change in the flow direction across the slot, resulting in amplification of the thermal diffusion from the plate along the flow. This change is suppressed by the flow acceleration due to a decrease in the channel width and, as seen in Figs. 2(c) and 3(c). The alternating change in the flow direction across the slot yields an increase in thermal diffusion from the rear plate, which is effected by the blockage factor. This thermal behavior becomes clearer for heat transfer performance from the rear plate.

Figure 4 illustrates, for Re=120, illustrates the time history of the Nusselt number, Nu, at one side wall of the rear plate. Note that numerical results during arbitrary time interval, i.e., of t=100 sec. to t=110 sec. are depicted in the figure, because the thermal transport phenomenon, from the calculation results, becomes periodic after about t=80 sec. Here, Nu implies the averaged Nusselt number over one side wall of the plate at each time, t. The oscillation of the heat transfer rate with time is caused by the alternating changes in the fluid flow across the slot, as mentioned previously. This mechanism of heat transfer enhancement is described in reference[23]. The Nusselt number is suppressed by a decrease in the channel width, i.e., an increase in the blockage factor, because the alternating changes in the fluid flow across the slot is attenuated due to the presence of the channel walls. In contrast, heat transfer rate is intensified in the narrow channel due to the substantial flow acceleration, in spite of the suppression of the alternating changes in the fluid flow. Furthermore, the oscillation of the heat transfer rate with time disappears in comparison with the wider channel flow case, as seen in Fig. 4. Heat transfer characteristics become clearer for the timewise variation of flow patterns and isotherms over both sides of the single-slot perforated plate.
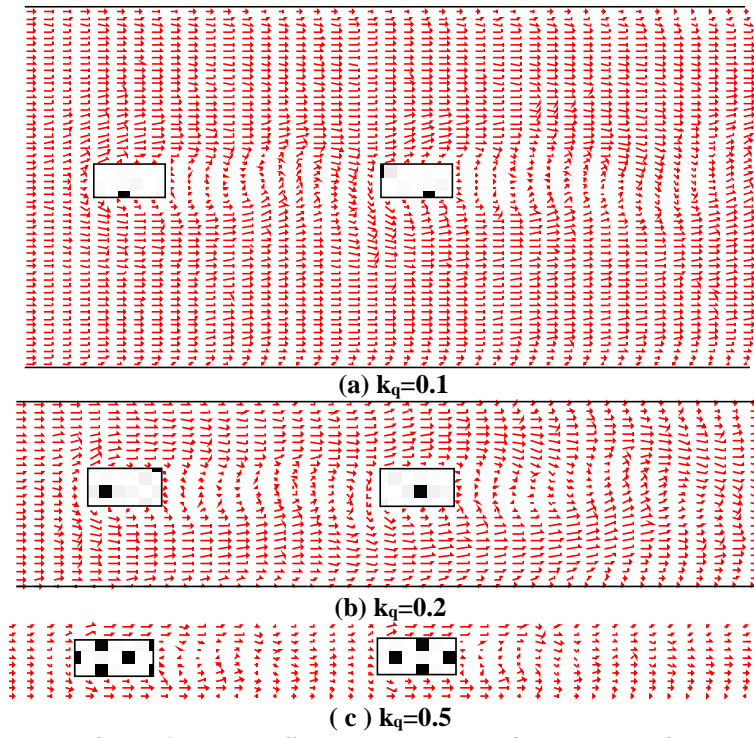
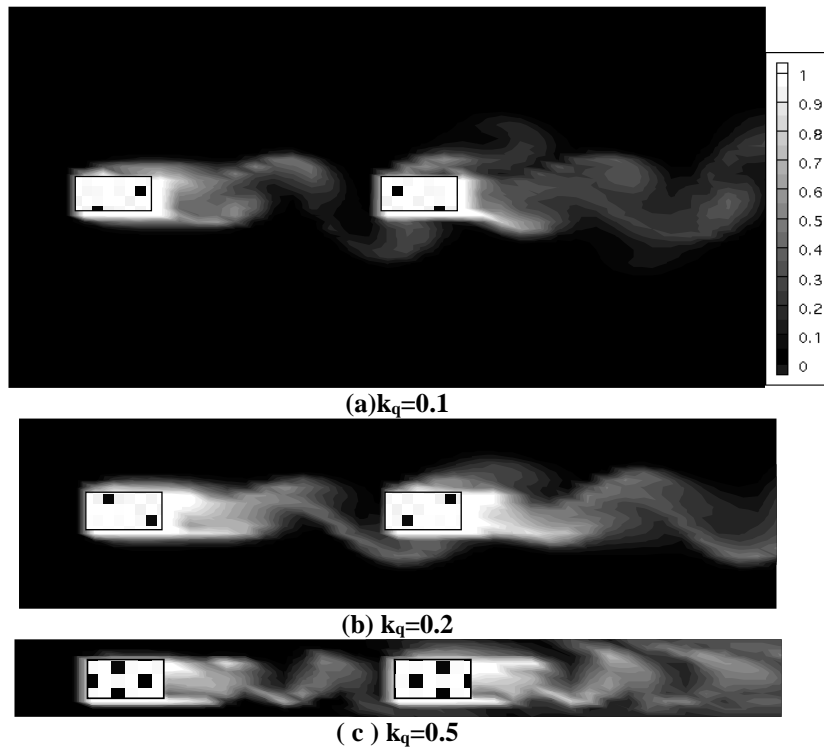**Fig. 2 Instantaneous maps of velocity-vector field around the perforated plate for Re=120 and t=100 sec.**

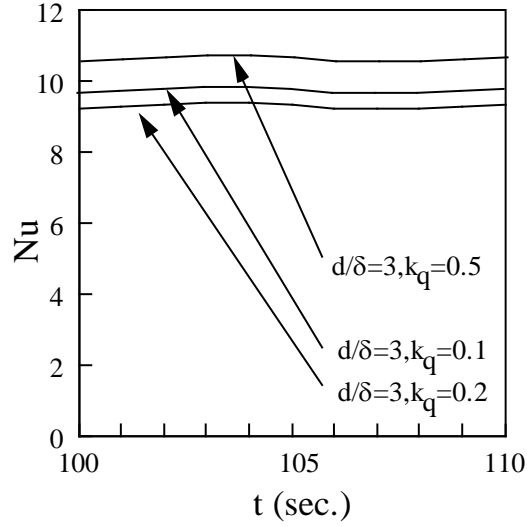**Fig. 3 Instantaneous maps of temperature field around the perforated plate for Re=120 and t=100 sec.**

Fig. 4 Timewise variation of Nusselt numbers at rear plate for Re=120.

The plot shows Nu (y-axis, 0 to 12) versus t (sec.) (x-axis, 100 to 110) with three curves labeled:
- $d/\delta=3, k_q=0.5$
- $d/\delta=3, k_q=0.1$
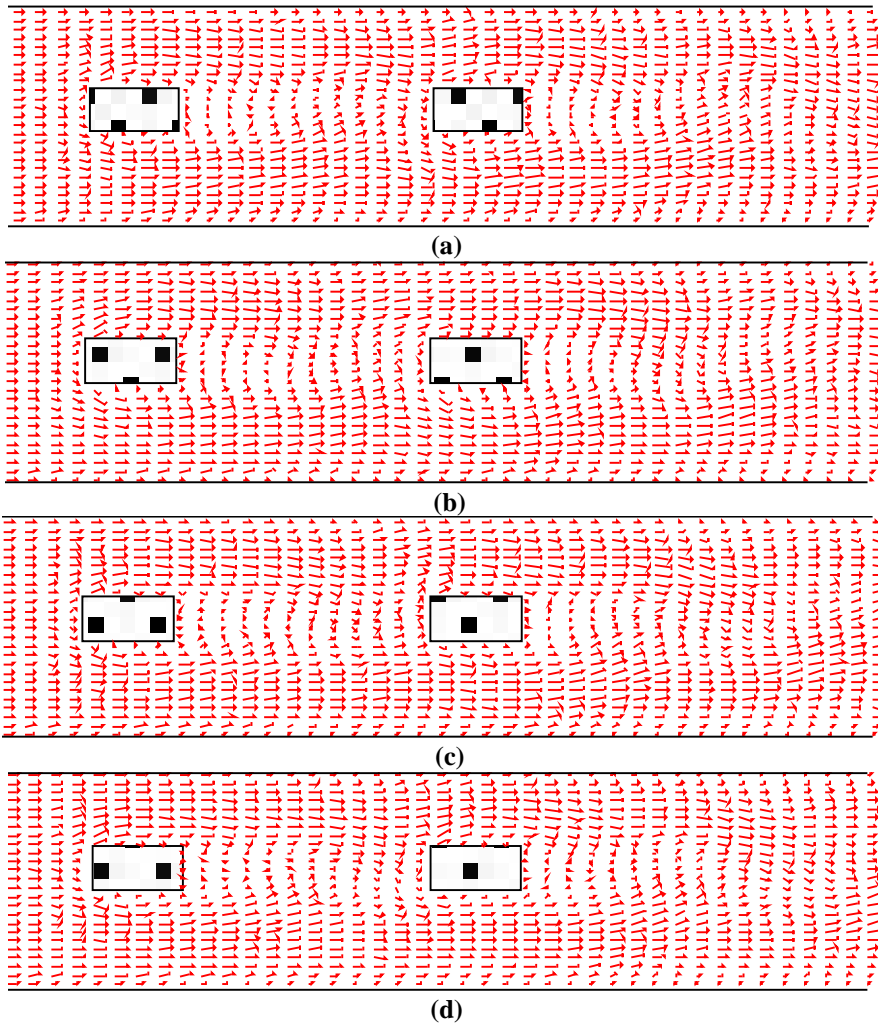- $d/\delta=3, k_q=0.2$

(a)

(b)

(c)

(d)

Fig. 5 Timewise variation of velocity-vector field around the perforated plate at a time interval of t=1.0 sec., for $k_q=0.2$ and Re=120.
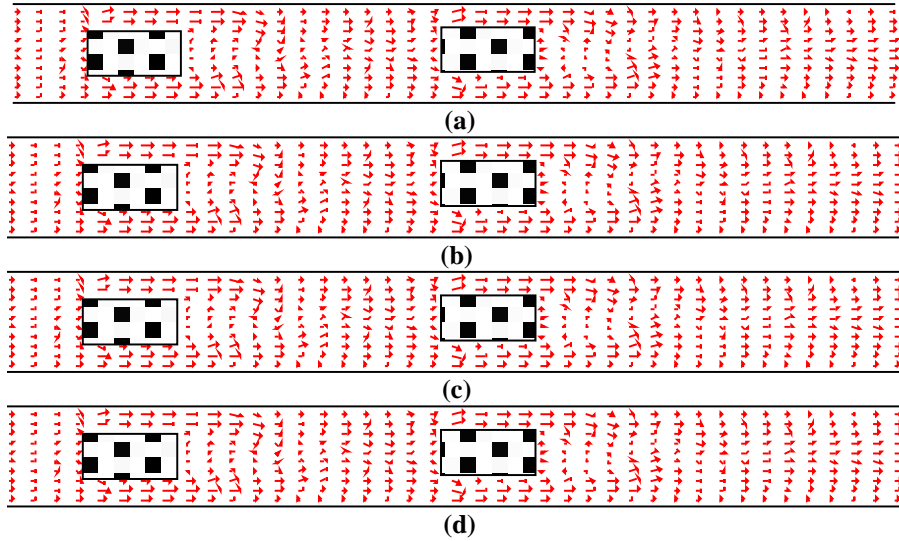
Fig. 6 Timewise variation of velocity-vector field around the perforated plate at a time interval of t=1.0 sec., for k_q=0.5 and Re=120.
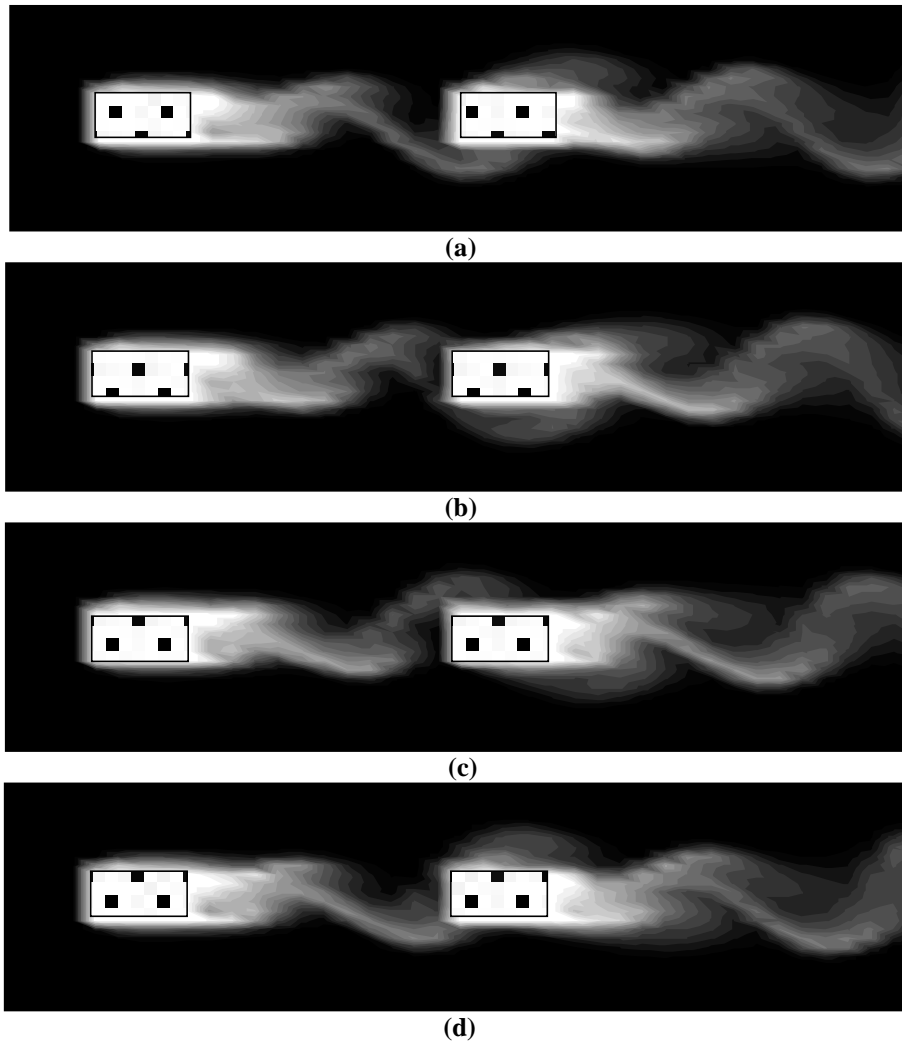

Fig. 7 Timewise variation of temperature field around the perforated plate at a time interval of t=1.0 sec., for k_q=0.2 and Re=120.
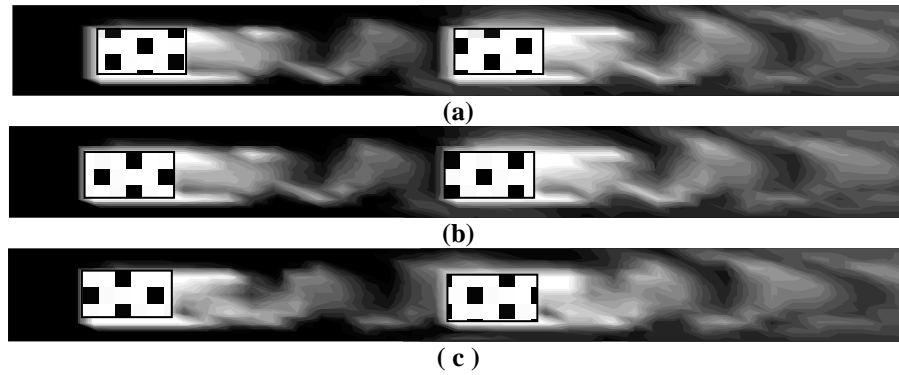
Fig. 8 Timewise variation of temperature field around the perforated plate at a time interval of t=1.0 sec., for $k_q=0.5$ and Re=120.

Figures 5 and 6 depict the timewise variation of flow patterns over both sides of the single-slot perforated plate. Consecutive images in Figs. 5 and 6 correspond to the numerical results for $k_q=0.2$ and $k_q=0.5$, respectively, and are obtained at a time interval of 1.0 sec. Notice that velocity components are normalized by dividing by inlet velocity, as mentioned previously. Figure 6 shows a sequence of alternating crossing of flow streaklines from one side of the plate to the other through the slot. On the contrary, the timewise variation of the flow streaklines is substantially attenuated due to the narrow channel, as shown in Fig. 6. The corresponding temperature distributions, i.e., isotherms are illustrated in Figs. 7 and 8. It is observed in Fig. 8 that the alternating change in the flow direction across the slot yields an increase in thermal diffusion from the rear plate. This results in a regular change in temperature distributions in the flow direction, particularly behind the rear plate. In contrast, such regular change occurs in the narrow channel flow (Fig. 8). It is found that (i) the alternating changes in the fluid flow, for $k_q=0.2$, result in an amplification of the heat transfer performance at the rear wall, as seen in Fig. 4, and (ii) further enhancement of heat transfer rate yields in the narrow channel flow, i.e., for $k_q=0.5$. This is because the flow is locally accelerated at the minimum cross-sectional area in the channel, so that the temperature gradient is substantially intensified in the vicinity of the heated plate.

Next task is to discuss the effect of the blockage factor on heat transfer performance from the slot-perforated plate. Figure 9 illustrates the time-averaged Nusselt number versus the Reynolds number with the blockage factor k_q, as a parameter. Although the Nusselt number is attenuated with an increase in the blockage factor, heat transfer performance is intensified in the substantially narrow channel, i.e., for $k_q=0.5$. This trend becomes larger in the lower Reynolds number region plotted. In other words, the effect of the blockage factor on heat-transfer performance becomes minor in the higher Reynolds number region. It is found that (i) as the channel width

becomes narrow, an alternating change in the velocity and temperature fields is suppressed, resulting in deterioration of heat transfer performance, and (ii) however, heat transfer enhancement is stimulated for larger blockage factor due to local acceleration at the minimum cross-sectional area in the channel. Notice that for lager blockage factor, the substantial pressure drop is needed to obtain the accelerated flow effect, that is the pressure loss increases.
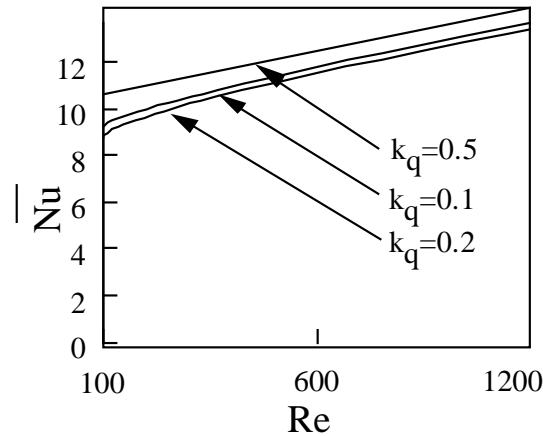

Fig. 9 Time-averaged Nusselt numbers for different blockage factor for $d/\delta=4$.

Attempt is made to obtain the optimum heat transfer performance by taking the pumping power into account. Figure 10, for Re=100, depicts the time-averaged Nusselt number on the plate fin against blockage factor, k_q and the corresponding dimensionless pressure drop $\Delta P'$ is superimposed in the same figure. It is observed that Nu increase with an increase in the blockage factor and the similar curve is shown for the pressure drop. In other words, the pressure drop is induced in the narrow space of the plate fins, as expected and its trend is attenuated in the wider spacing. It is noted, for the k_q range considered here, that the Nusselt number increases to 20%, while the pressure drop amplifies to 240%. This indicates that the optimum heat transfer performance is obtained by suppressing an increase in the pressure drop, that is, higher thermal performance yields at $k_q=0.4$.
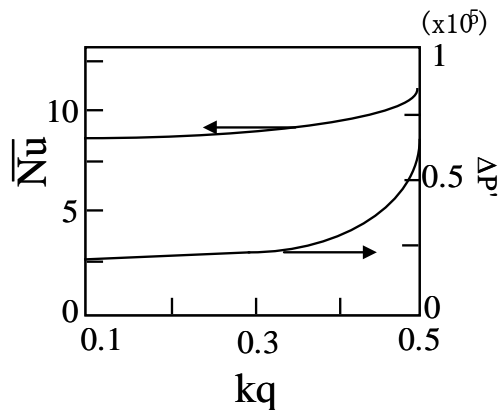

Fig. 10 Hydrodynamic and thermal performance for Re=100.

IV. Summary

A numerical and experimental study has been performed on unsteady thermal-fluid flow over a perforated plate (consisting of two plates spaced at an interval of d in the flow direction) installed in channels with different widths. Consideration was given to the roles of the Reynolds number and the blockage factor on the flow and temperature fields. It was found that:

1. An alternating changes in the fluid flow results in an amplification of the heat-transfer performance at the rear wall.

2. When the channel becomes narrower, the alternating change in the fluid flow is suppressed, resulting in an attenuation of the heat-transfer performance at the rear wall of the rear plate.

3. Heat transfer enhancement is stimulated for larger blockage factor due to local acceleration at the minimum cross-sectional area in the channel, whose trend becomes larger in the lower Reynolds number region considered here.

References

[1]Wong, S, Duncan, J. D. Gibson J. C., and Killackey, J. J., "Compact Condenser for Rankine Cycle Engine," Final Report 71-7464, (Prepared for Environmental Protection Agency), Air Research Manufacturing Co. Calif., 971.

[2]Kays, W. M., "The Heat Transfer and Flow Friction Characteristics of a Wave Fine, a Strip Fin, and a Perforated Fin Heat Transfer," No. 39, Dep. Mech. Eng., Stanford Univ., Stanford, Calif., 1958.

[3]Shah, R. H. and Osborn, H. H., "Final Report-Advanced Heat Exchanger Design of Compact Heat Exchanger When Operating in a Marine Environment," Air Preheat Company, Wellesville, New York.1967.

[4]Liang, C. Y. and Yang, W.-J., "Heat Transfer and Friction Loss Performance of Perforated Heat Exchanger Surface," *ASME Heat Transfer Conf.*, Vol. 97, 1975, pp. 9-15.

[5]Liang, C. Y. and Yang, W.-J., "Modified Single Blow Technique for Performance Evaluation on Heat Transfer Surface, *ASME Heat Transfer Conf.*, Vol. 97, 1975, pp. 16-21.

[6]Liang, C. Y., Yang, W.-J., and Hung, Y. Y., "Perforated-Fin Type Compact Heat Exchangers for Gas Turbines," *Tokyo Joint Gas Turbine Congress,* 1977, pp. 77-85.

[7]Lee, C. P. and Yang, W.-J., "Augmentation of Convective Heat Transfer from High-Porosity Perforated Surfaces," *Heat Mass Transfer 1978-Toronto*, Vol. 2, 1978, pp. 589-594.1978.

[8]Fujii, M., S. Seshimo, S., and Yamanaka, G., "Heat Transfer and Pressure Drop of Perforated Surface Heat Exchanger with Passage Enlargement and Contraction," *International Journal of Heat Mass Transfer*, Vol. 31, 1988, pp. 135-142.

[9]Hwang, G. J., Wu, C. C., Lin, L. C., and Yang, W.-J., "Investigation of Flow Drag and Forced Convective Heat Transfer in Perforated Coolant Channels," *Transport Phenomena in Combustion*, edited by S. H. Chan, Vol. 2, Taylor & Francis, 1996, pp. 1747-1758.

[10]Liang, C. Y., "Heat Transfer, Flow Friction, Noise and Vibration Studies of Perforated Surface," Ph. D. Dissertation, University of Michigan, Ann Arbor, MI.1975.

[11]Liang, C. Y., Lee, C. P., and Yang, W.-J., "Visualization of Fluid Flow Past Perforated Surfaces," *Proc. Japanese 4th Symp. Flow Visualization,* 1976, pp. 69-73.

[12]S. Torii and W.-J. Yang, 1998, Numerical Flow Visualization of a Slot-Perforated Flat Surface in Free Stream, 1998-CSME, 1, 177-184.

[13]S. Torii and W.-J. Yang, 1998, Flow over a Slot-Perforated Flat Surface between Two Parallel Plates, Proceedings of 8th International Symposium of Flow Visualization, No.006, 1-8.

[14]Torii, S., Yang, W.-J., and Umeda, S., "Flow Visualization and Transport Phenomena over a Slot-Perforated Flat Surface between Two Parallel Plates," *J. Flow Visualization and Image Processing*, Vol. 5, 1998, pp. 63-80.

[15]Amon, C. H., and Mikic, B. B., "Spectral Element Simulations of Unsteady Forced Convective Heat Transfer: Application to Compact Heat Exchanger Geometries," *Numerical Heat Transfer*, Part A, Vol. 19, 1991, pp.1-19.

[16]Suzuki, K., Xi, G. N., Inaoka, K., and Hagiwara, Y., "Mechanism of Heat Transfer Enhancement due to Self-Sustained Oscillation for In-Line Fin Array," *Int. J. Heat Mass Transfer*, Vol. 37, 1994, pp. 83-96.

[17]Nigen, J. S., and Amon, C. H., "Time-Dependent Conjugate Heat Transfer Characteristics of Self-Sustained Oscillatory Flows in a Grooved Channel," *J. Fluid Engineering*, Vol. 116, 1994, pp. 499-507.

[18]Kim, S. H., and Anand, N. K., "Use of Slots to Enhance Forced Convective Cooling between Channels with Surface-Mounted Heat Sources", *Numerical Heat Transfer*, Vol. 38, 2000, pp. 1-21.

[19] Zukauskas, A., and Ziugzda, J., *Heat Transfer of a Cylinder in Crossflow*, Hemisphere Publishing Corporation. 1985.

[20]Harlow, F. H., and Welch, E. J., "Numerical Calculation of Time-Dependent Viscous Incompressible Flow of Fluid with Free Surface," *Phys. of Fluids*, Vol. 8, 1965, pp. 2182-2189.

[21]Hirt, C. W., Nichols, B. D., and Romero, N. C., "SOLA-A Numerical Solution Algorithm for Transient Fluid Flows," LASL Report, LA-5852.1975.

[22] Torii, S., Yang, W.-J., and Umeda, S., "Flow Visualization and Transport Phenomena over a Slot-Perforated Flat Surface between Two Parallel Plates," *J. Flow Visualization and Image Processing*, Vol. 5, 1998, pp. 63-80.

[23] Torii, S., and Yang, W.-J., "Thermal Fluid Transport Phenomena over Slot-Perforated Flat Surface in Channels," *J. Flow Visualization and Image Processing*, Vol. 9, 2002, pp. 281-285.